

Coupled-channel-Born-approximation study of (p, t) reactions leading to two-phonon states of vibrational nuclei*

T. Udagawa

Center for Nuclear Studies, University of Texas, Austin, Texas 78712

(Received 2 July 1973)

A coupled-channel-Born-approximation (CCBA) study is made of (p, t) reactions leading to two-phonon states of vibrational nuclei. A detailed numerical analysis is performed, particularly for the $^{116}\text{Cd}(p, t)^{114}\text{Cd}$ reaction with the incident energy $E_p = 28$ MeV. It is shown that many features observed in the reactions, which cannot be explained by the distorted-wave Born approximation (DWBA), can successfully be accounted for by CCBA. It is also shown that three-step processes play an essential role in the successful explanation of the observed data, particularly the cross sections of the 0^+ and 4^+ two-phonon states.

[NUCLEAR REACTIONS $^{116}\text{Cd}(p, t)$, $E = 28$ MeV; calculated $\sigma(\theta)$.]

I. INTRODUCTION

The two-nucleon transfer reaction has proved to be a very useful tool in obtaining nuclear structure information, particularly on the correlations of the transferred pair in the nucleus and also collective modes associated with these pair correlations.¹ Actually, by utilizing this reaction, many pairing-vibrational states were identified in near-magic nuclei, which may be one of the most important successes of this new reaction method.¹ Of course the reaction can be, and indeed has been, applied to study the nuclear structure of many other classes of nuclear excitation.

So far most of these studies of the two-nucleon transfer reactions were based on the distorted-wave Born approximation (DWBA),² which assumes a direct, single-step mechanism for the two-nucleon transfer process. Recent experimental evidence, however, suggests that the single-step mechanism is not necessarily the dominant reaction mechanism of the two-nucleon transfer reaction. For example, angular distributions of the (p, t) reaction leading to the first excited 2^+ (2_1^+) state of rotational³ and vibrational⁴ nuclei are often found to show an angular pattern which is quite different from that of an $L = 2$ DWBA calculation. Unnatural-parity states, which are not allowed to be excited via direct, single-step mechanism, are also found to be excited rather strongly.⁵ These observations demonstrate that a multistep process plays an important role in the two-nucleon transfer reaction.

Theoretically, it has become feasible recently to calculate multistep processes arising from the inelastic scattering processes within the framework of the coupled-channel-Born-approximation (CCBA)

formalism.^{6,7} Thus, Glendenning and his collaborators⁸ have performed CCBA calculations of (p, t) reactions on some of vibrational nuclei, demonstrating that the effects are quite important. The same authors⁹ and also Tamura *et al.*¹⁰ then made CCBA analysis of actual observed data of the (p, t) reactions on deformed nuclei,³ explaining successfully the observed anomaly of the 2_1^+ angular distribution mentioned above. Yagi *et al.*⁴ also made a similar analysis of the (p, t) reaction on vibrational nuclei, obtaining the same success. Further, it was shown that the excitation of unnatural-parity states in the $^{22}\text{Ne}(p, t)^{20}\text{Ne}$ reaction⁵ can also be explained well by CCBA.¹¹

In the present work, we extend such CCBA studies of the (p, t) reaction to those leading to the two-phonon states of vibrational nuclei. The experimental data to be used have recently become available due to Comfort *et al.*,¹² who did a very accurate measurement of the cross section of these two-phonon states for three cases, $^{112, 114, 116}\text{Cd}(p, t)^{110, 112, 114}\text{Cd}$.

The analysis of the above data for the two-phonon states is particularly interesting since it provides a further detailed test of CCBA; indeed, as is expected and also will later be shown, three-step processes play a very essential role in the excitation of the two-phonon states. This was not so in the cases studied before, where the two-step processes are the dominant processes among the various conceivable multistep processes. Therefore, one can test up to the next higher order in the CCBA amplitude in the present case.

In addition to interest from the point of view of reaction mechanism, the study of the reaction is also interesting from the nuclear structure point of view. The structure of the two-phonon states,

particularly their detailed dynamical nature, is not well known yet, in spite of the fact that a great number of papers have so far been devoted to the study of this subject. This might partly be due to the fact that we have not enough experimental means to explore these states; indeed, the dynamical nature of the states has so far been studied only by means of inelastic scattering¹³ and Coulomb excitation,¹⁴ which tell us only the particle-hole (p-h) correlation aspect of the state. The two-nucleon transfer reactions can provide supplemental information which is thus very valuable. However, in order that such a spectroscopic study of the (p, t) reaction become feasible, one must have a reaction theory which can really describe the reaction mechanism. It is the aim of the present work to show that CCBA, together with a phenomenological microscopic model of nuclear structure, can indeed describe fairly well the observed data of the (p, t) reaction.

In Sec. II we first summarize the experimental data that are to be analyzed in the present work. A few remarks are given on the data, particularly on those aspects which cannot be explained by DWBA. In Sec. III a discussion is given of the form factors that are used in the present calculations. We introduce a rather phenomenological treatment of the form factors used in the calculation, which is given in detail in this section, together with the results of the actual evaluation of the form factors. Sec. IV is devoted to a discussion of the optical-potential parameters used in the present calculations. Results of actual numerical calculations are then shown in Sec. V, where the results are also compared with experiment. Finally, in Sec. VI concluding remarks are given.

II. EXPERIMENTAL DATA

We summarize in this section the experimental materials that are to be analyzed here, and give a brief discussion on them. As was already mentioned in the introduction, we utilize the data taken by Comfort *et al.*,¹² who measured the cross sections of (p, t) reactions from three Cd target nuclei, $^{112}, ^{114}, ^{116}\text{Cd}$. The incident energy used was $E_p = 27.9$ MeV. In the actual experiments the measurement of the cross sections was made for various final states up to 3-4-MeV excitation energy. In the present work, however, we are only interested in the cross sections of the ground 0^+ (0_g^+), the one-phonon 2^+ (2_1^+), and the two-phonon 0^+ (0_1^+), 2^+ (2_2^+), and 4^+ (4_1^+) states.

The experimental cross sections of these states obtained for three cases of target nuclei are all summarized in Figs. 1 and 2, separately for each

final spin state. In Fig. 1, the cross sections of the 0_g^+ , 2_1^+ , 2_2^+ , 4_1^+ states are presented. Now, we observe one remarkable feature in Fig. 1, which is that if the final spin state is fixed all the cross sections taken for these different target nuclei have almost the same magnitude as well as the shape. There is one exception to this, which is seen in the 2_2^+ cross section of the $^{112}\text{Cd}(p, t)-^{110}\text{Cd}$ reaction. In this case the cross section is

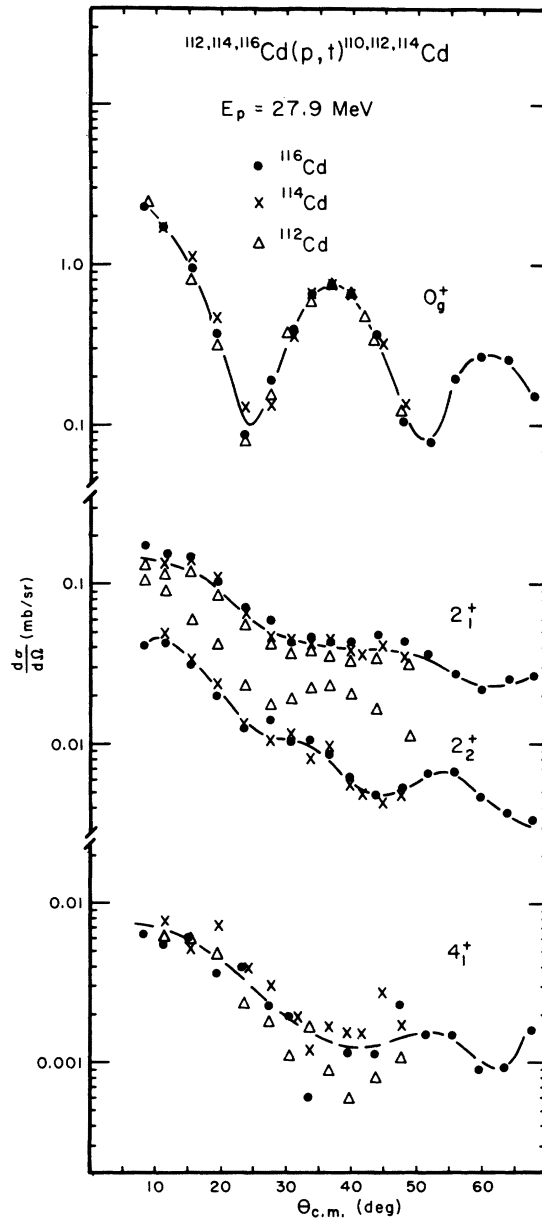


FIG. 1. Experimental differential cross sections for (p, t) reactions leading to the 0_g^+ , 2_1^+ , 2_2^+ , and 4_1^+ states in $^{114-110}\text{Cd}$.

somewhat larger than the two other 2_2^+ cross sections. This might, however, be due to the fact that the 2_2^+ state is a doublet with the 0_1^+ state¹⁵ and therefore the observed cross section would involve some amount of the 0_1^+ cross section. If one really assumes that this is the case, i.e., that the 2_2^+ cross section of ^{110}Cd is the same as those of the two other 2_2^+ states, one can estimate the 0_1^+ cross section by subtracting from the observed data an average 2_2^+ cross section of the neighboring nuclei. The 0_1^+ cross section for ^{110}Cd given in Fig. 2 is estimated in this way.

Now, the similarity observed in the 0_g^+ , 2_1^+ , 2_2^+ , and 4_1^+ cross sections and demonstrated clearly in Fig. 1 seem to indicate that the wave functions of these states are more or less very similar for all the Cd isotopes concerned. This is also consistent with evidence obtained from other experimental data, such as the energies and also the various $E2$ transition rates.¹⁴ The above similarity further suggests that it is enough, for the purpose of the present work, to carry out the calculations only for one example of the reactions, particularly for 0_g^+ , 2_1^+ , 2_2^+ , and 4_1^+ states because if a reasonable explanation is established for one

case, it can be applied to other cases literally. In the present work, we actually perform the calculations specifically for the $^{116}\text{Cd}(p,t)^{114}\text{Cd}$ reaction.

In contrast to the 0_g^+ , 2_1^+ , 2_2^+ , and 4_1^+ cross sections, the 0_1^+ cross sections shown in Fig. 2 exhibit a rather dramatic but regular change in both their shape and magnitude with the target mass number. The angular pattern of the cross sections shifts to forward angles, accompanying an increase of the magnitude with decreasing mass number. The observed change in the cross section, particularly the change of the shape with the mass number, cannot of course be explained by DWBA.

In connection with this it may be interesting to note that the position of the deep minimum observed at about 34° in the 0_1^+ cross section of the $^{116}\text{Cd}(p,t)^{114}\text{Cd}$ reaction is very close to the maximum (observed at about 36°) of the 0_g^+ cross section. This implies that the angular distribution of the 0_1^+ cross sections looks almost out of phase to that of 0_g^+ . This feature also cannot be explained by DWBA.

Besides the points discussed above, there are at least three other remarkable features that are also difficult to explain by DWBA: (i) There is a marked difference between the two 2^+ (2_1^+ and 2_2^+) cross sections; (ii) the angular distribution of the 4_1^+ state is very different from that of the $L=4$ DWBA (which are calculated for instance in Ref. 16), and (iii) the 2_1^+ cross section also shows an angular pattern which is different from an $L=2$ DWBA.¹² We shall show later that all these features in the observed cross sections are explained very well by CCBA.

While not directly related to the difficulty with which DWBA meets, it might be worthwhile to note here that the two-phonon 2^+ cross section is larger by about a factor of 5 than those of other two-phonon 0^+ and 4^+ states. We shall try to give a possible explanation of this feature of the observed data.

III. FORM FACTORS

A. Preliminary remarks

As was already mentioned in the introduction, we introduce a rather phenomenological treatment of the form factors used in the present CCBA calculations. Thus, we first outline it before going into details of the actual numerical calculations, which are performed in the following subsection (III B). From consideration of the angular momentum and parity conservation, we expect to have 45 nonvanishing form factors in all between the ground, one-phonon, and two-phonon states of the initial target and final residual nuclei. At the

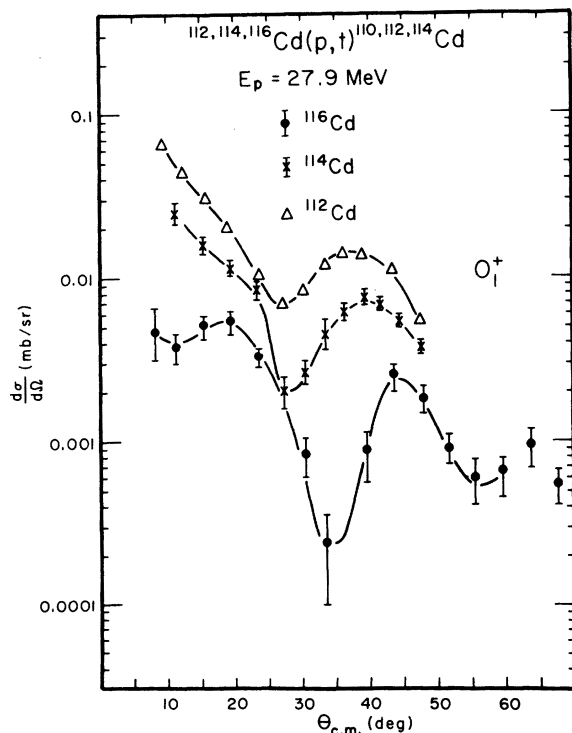


FIG. 2. Experimental differential cross sections for (p, t) reactions leading to 0_1^+ states of $^{114-110}\text{Cd}$. The 0_1^+ cross section of the ^{110}Cd was extracted from the doublet peak of the observed data in a manner explained in the text.

present moment, it is very difficult to derive all these form factors unambiguously, particularly those related to the two-phonon states, since the wave functions of these states are not well known.

Thus, we are more or less forced to introduce an approximation for the treatment of the form factors. The approximation that we particularly use in this work is that we start with the following set of 7 form factors (we call it conveniently set I), i.e., 5 $L=0$ form factors of transitions between the same I_n^+ states of both the initial and final nuclei, and 2 $L=2$ form factors of the $0_g^+-2_1^+$ and $2_1^+-0_g^+$ transitions. Other form factors are then treated as phenomenological, to be fixed from experiments; namely, additional form factors are introduced only when they are required in order to obtain a better fit to experiment.

As will be shown later, however, most of the experimental data can be reproduced very nicely without introducing any additional form factor. Thus, most of the calculations in the present work are performed by using only the form factors of the set I. When an additional form factor is introduced, however, it will be explained at the stage when it is actually used.

The above choice of starting form factors was made based on the fact that these are the ones expected to be very important. Particularly, this is so for the $L=0$ form factors for the reason that the neutrons in Cd isotopes considered here are in a superconductive state.^{1,17} These form factors may then be calculated by using the BCS wave functions derived from a simple pairing-force model, which enjoyed some success to explain observed collective features of (p, t) reactions.¹ As will be discussed later (Sec. III B), we indeed calculate the $L=0$ form factors with a wave function which is essentially the same as that of BCS.

Before proceeding, we want to remark on the $L=2$ form factors considered above, particularly on the form factor of the direct, $0_g^+-2_1^+$ transition. As will be shown later, the calculated form factor turned out to be very small, implying that the direct 2_1^+ excitation is very weak. Also, the calculation involves a fairly large theoretical uncertainty. Due to this, we show also in the present work calculations which include all the form factors of the set I, except the direct, $0_g^+-2_1^+$ transition form factor; we call this set of form factors, which exclude the direct $0_g^+-2_1^+$ form factor, set II.

Another remark that might be worthwhile to make here is that the smallness of the direct, $0_g^+-2_1^+$ form factor justifies the present approximate treatment of the form factors. The direct 2_1^+ excitation is the process that creates a phonon during the (p, t) processes. The smallness of the

form factor of this phonon-creation process simply means that the form factor for the one-phonon-to-two-phonon-state transitions will also be small. Further, it is physically reasonable to consider that the direct excitation of the two-phonon states from the target ground state by the (p, t) process should be small.^{8,12}

B. Calculations

In order to calculate the form factor, use is made of a formula²

$$F_L(I_n^+ - I_m^+; r) = \begin{cases} \sum_N G_N u_{NL}(r) & r \leq r_m \\ h_L(r) & r > r_m, \end{cases} \quad (1)$$

where $u_{NL}(r)$ is the harmonic-oscillator (H.O.) wave function, $h_L(r)$ the Hankel function, and G_N the structure function that carries all the nuclear structure information, and is calculated from nuclear wave functions. As is seen, the form factor is constructed first with help of the H.O. wave function in the interior region of the nucleus, which is then joined smoothly onto a Hankel function at appropriate radius r_m .

In order to calculate the G_N factor, we assume in this work wave functions of the 0_g^+ and 2_1^+ states which are very similar to those used before¹⁸ to describe those states in ¹⁴⁰Nd which have two neutron holes. The nucleus considered now has two proton holes, instead of the two neutron holes, but the wave functions may be given in a very similar manner as¹⁹

$$|0_g^+\rangle = [\alpha_1 B_0^\dagger + \alpha_2 (B_2^\dagger C_2^\dagger)_0 + \alpha_3 B_0^\dagger (C_2^\dagger C_2^\dagger)_0] |0\rangle, \quad (2a)$$

$$|2_1^+\rangle = [\gamma_1 B_2^\dagger + \gamma_2 B_0^\dagger C_2^\dagger + \gamma_3 (B_2^\dagger C_2^\dagger)_{12}] |0\rangle. \quad (2b)$$

Here B_0^\dagger and B_2^\dagger are, respectively, the creation operators of the 0^+ and 2^+ pairing-vibrational phonons that describe the excitations of the two-proton holes, while C_2^\dagger is the creation operator of the collective, p-h vibrational phonon. This p-h vibrational phonon represents the excitation of the core, the rest of the nucleus other than the two-proton holes. Since the proton shell is closed, the excitation of the core is of course mainly due to that of the neutron in the open shell. The p-h phonon, C_2^\dagger , is thus mainly made of the neutron two-quasi-particle states. $|0\rangle$ in Eq. (2) is a vacuum state of the phonons and describes the ground state of the core. Except for the ground-states correlations created by our use of random-phase approximation (RPA) in constructing the phonon operators (see the discussion given below), $|0\rangle$ essentially describes the proton closed-shell

TABLE I. Single-particle states and their energies used in the wave function and form factor calculations. The pairing-force strengths of the monopole and quadrupole types, (G), as well as the Q - Q forces, (F) are also listed in the table.

	Proton		Neutron	
	l_j	E_{lj} (MeV)	l_j	E_{lj} (MeV)
	$0f_{5/2}$	-5.41	$0f_{5/2}$	-5.53
	$1p_{3/2}$	-3.01	$1p_{3/2}$	-5.10
	$1p_{1/2}$	-2.71	$1p_{3/2}$	-4.80
	$0g_{9/2}$	-2.41	$0g_{9/2}$	-4.50
	$1d_{5/2}$	2.95	$1d_{5/2}$	0.0
	$0h_{11/2}$	4.35	$0g_{7/2}$	0.25
	$1d_{5/2}$	5.05	$2s_{1/2}$	2.18
	$2s_{1/2}$	5.37	$0h_{11/2}$	2.24
			$1d_{3/2}$	2.50
			$1f_{7/2}$	6.40
			$2p_{3/2}$	7.30
			$0h_{9/2}$	8.30
			$1f_{5/2}$	10.20
			$2p_{3/2}$	12.50
			$0i_{13/2}$	15.50
G_0 (MeV)	0.180		0.128 (^{114}Cd)	0.135 (^{116}Cd)
G_2 (MeV)	0.096		0.135 (^{116}Cd)	
F_2 (MeV)	0.050		0.045	
$F_2^{\eta p}$ (MeV)		0.060	0.050	

core and the neutrons in BCS vacuum state.

All the phonon operators are obtained by using RPA, together with the simple quadrupole-quadrupole (Q - Q) and the (monopole and quadrupole) pairing-force model. The mixing of various components in the wave functions of Eqs. (2a) and (2b) is then derived by diagonalizing the H_{31} term of the Q - Q interaction, which has not been taken into account in constructing the phonon operators, C_2^+ , B_0^+ , and B_2^+ .¹⁸ With these approximations, and also with the help of the parameters listed in Table I, the coefficients in Eq. (2) were found to be $\alpha_1 = 0.82$, $\alpha_2 = 0.40$, $\alpha_3 = 0.18$, $\gamma_1 = 0.63$, $\gamma_2 = 0.64$, and $\gamma_3 = 0.16$. The structure factors of the $0_g^+ \rightarrow 0_g^+$, $0_g^+ \rightarrow 2_1^+$, and $2_1^+ \rightarrow 0_g^+$ transitions obtained by using the above wave functions are presented in Table II. The form factors of these transitions will then be calculated by using Eq. (1).

The form factors of other $L=0$ transitions (between one-phonon and also two-phonon states) may be obtained from the $0_g^+ \rightarrow 0_g^+$ transition form factor

[we denote it by $F_0(\tau)$] by making a correction due to the blocking effect, which originates from the presence of the quasiparticles in the excited phonon states, reducing somewhat the magnitude of the form factor. The importance of the blocking effects in the (p, t) processes was recently noted in (p, t) on odd- A nuclei.²⁰ The form factors may then be written by

$$F_0(I_n^+ - I_n^+; \tau) = b_n(I_n^+)F_0(\tau), \quad (3)$$

where b describes the blocking effect. We made a rough estimation of the b value for the 2_1^+ state by using the 2_1^+ -state wave function of Eq. (2b). We then get $b(2_1^+) = 0.85$. For the case of the two-phonon states the b value might be somewhat smaller, but here we simply assume that the b values are the same as that of the one-phonon state.

The following remarks may be worthwhile here:

(i) The calculated $L=2$, G_N factors are rather small, particularly for the $0_g^+ \rightarrow 2_1^+$ transition. This means that the strength of the direct 2_1^+ excitation is weak; indeed we shall show later that the DWBA predicts a too small cross section to explain the observed cross section. This weakness of the direct 2_1^+ excitation results from the fact that the effects of the ground state correlations contribute destructively for the (p, t) transition processes. This is in contrast to the effect on the $E2$ transition rate.¹⁷ Another reason for the reduction is that the 2_1^+ state has significant mixing of the proton configuration [the first term in Eq. (2b)] which does not contribute to the (p, t) transition. (ii) For reasons discussed above, the form factor for the direct transition strength to the 2_1^+ state becomes very small. Moreover, it is rather sensitive to the details of the parameters involved in the calculations. Thus, for instance, if one changes the position of the $h_{11/2}$ single-particle state by about 300 keV, the form factor changes its value by about 15%. The form factor is also sensitive to the values of the strength parameters of the Q - Q force or quadrupole pairing force. Because of this we performed for this work calculations which assume another set of form factors (we call it the set II), which neglect the form factor of the direct 2_1^+ -excitation form factors of the set I, as mentioned earlier.

TABLE II. Calculated structure factors G_N for $L=0$, $0_g^+ \rightarrow 0_g^+$ and $L=2$, $0_g^+ \rightarrow 2_1^+$ and $2_1^+ \rightarrow 0_g^+$ transitions.

N	0	1	2	3	4	5	6
$0_g^+ \rightarrow 0_g^+$	0.0064	-0.0184	0.0681	-0.2497	0.6308	-0.1953	0.00262
$0_g^+ \rightarrow 2_1^+$	0.0008	-0.0039	0.0165	-0.0669	0.0008		
$2_1^+ \rightarrow 0_g^+$	-0.0018	0.0061	-0.0231	0.1676	-0.0321		

IV. OPTICAL POTENTIAL PARAMETERS

In the present CCBA calculation, use is made of a deformed-vibrational optical-potential model¹³ to generate the CC distorted waves. As is usually done, we use insofar as possible optical-potential parameters, which are determined from the analysis of the elastic and inelastic scattering data.²¹⁻²⁵ The parameters actually used in the present calculations are summarized in Table III.

Strictly speaking, however, the procedure of fixing the optical-potential parameters by the elastic and inelastic scattering data can be justified only for the case of reactions in which the angular momentum mismatch is comparable with the actual angular momentum transfer so that the partial waves well defined by the elastic and inelastic scattering data dominantly contribute to the reaction cross sections.

Unfortunately this is not the case for the present reaction. To demonstrate this, we present in Fig. 3 a diagram of the absolute magnitude of the reflection coefficient,²⁶ $|\eta_l|$, as a function of the orbital angular momentum, l , for both the proton and triton, together with the overlap integral, $|I_l|$, multiplied by $(2l+1)^{1/2}$ for the $L=0$, $0_g^+ - 0_g^+$ transition. As is seen from Fig. 3, the value reaches its half value at $l \approx 7$ for the proton, and $l \approx 12$ for

TABLE III. Optical-potential parameters used in the present CCBA calculations. The notation used in this table is the same as that of Refs. 13 and 22.

	P	t
V	56.3	170.0
W	2.9	19.0
W_D	6.7	...
r	1.22 (1.17)	1.15
r_I	1.32	1.52
r_D	1.32	...
r_c	1.25	1.40
a	0.75	0.74
a_I	0.62	0.76
a_D	0.62	...
$W_c^{(1)}$	0.8	0.8
$W_c^{(2)}$	1.0 or 0.8 ^a	1.0 or 0.8 ^a
$W_c^{(3)}$	1.0	1.0
β_{02}	0.17	0.09 ^b or 0.13 ^c
β_{20}	+0.125	0.07
β_{00}^{11}	-0.006	-0.012
β_{22}	+0.13	0.09
β_{02}^{11}	0.05	0.05
β_{24}	0.13	0.070
β_{04}^{11}	0.02	0.00

^a Used for $0_g^+ - 2_1^+ - I_n^+$ coupling calculation.

^b Set I.

^c Set II.

the triton, respectively. The angular momentum mismatch is thus found to be 5, which is much larger than the angular momentum transfer for the $L=0$ or $L=2$ transitions. Due to this, the overlap integral $|I_l|$ has its maximum value for triton partial waves which are not well defined by the elastic scattering, although proton partial waves that give the maximum overlap integral are still in the region well defined by the elastic scattering. This feature is also seen in Fig. 3.

The above result shows that the triton waves that contribute to the reactions cannot be well defined by the elastic and inelastic scattering data, and therefore there is an ambiguity for the choice of the parameters. Actually, we treated the deformation parameter of $0_g^+ - 2_1^+$ inelastic coupling as an adjustable parameter and determined the value in such a way that the calculated CCBA 2_1^+ cross section fits the observed data. The values determined in this way are $\beta_2 = 0.09$ and 0.13 according to the choice of the form factor set I and II, respectively.

Finally, we remark here that we use a fixed value of the zero range parameter, $D_0^2 = 4.8 \times 10^4$

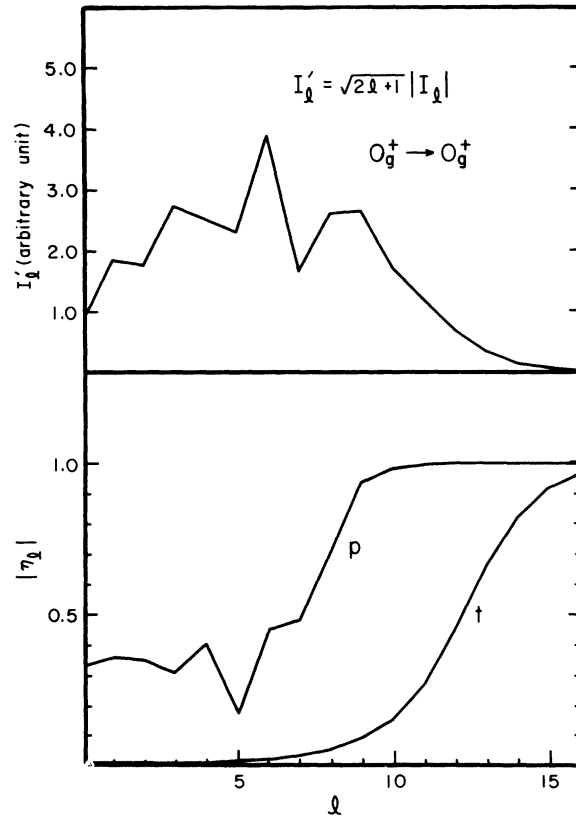


FIG. 3. Reflection coefficients of proton and triton elastic scattering. The DWBA radial-overlap integrals are also shown.

$\text{MeV}^2 \text{fm}^3$, for all calculations performed here. This value was actually determined by fitting the calculated CCBA 0_g^+ cross section to experiments as we shall discuss later in Sec. V A.

V. RESULTS OF CCBA CALCULATIONS AND COMPARISON WITH EXPERIMENTAL DATA

We discuss in this section the CCBA calculations and compare the results with experiments. A computer code MARS is used for this purpose.²⁷ The inelastic coupling to the two phonon states is neglected in computing the cross section to the 0_g^+ and 2_1^+ states, while a $0_g^+-2_1^+-I_n^+$ coupling is used when the cross sections of the two-phonon spin-1 state are calculated.

A. Ground-state cross section

In Fig. 4, we show the results of the CCBA calculations for the 0_g^+ state, together with the experimental data. As is seen, the shape of the experimental cross section is well reproduced by the calculations. The absolute magnitude is also well reproduced with the help of the zero-range parameter, $D_0^2 = 4.8 \times 10^4 \text{ MeV}^2 \text{fm}^3$ assumed before. This zero-range parameter is used for all the calculations discussed henceforth.

It might be worthwhile to note here that the

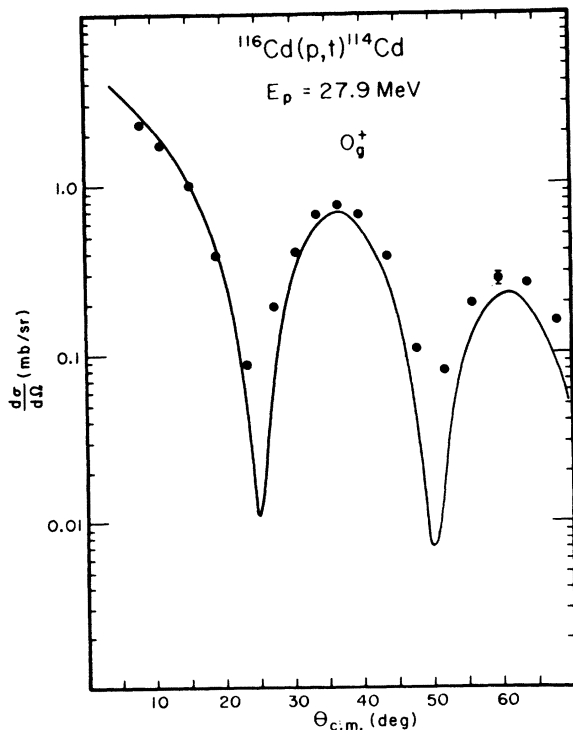


FIG. 4. Calculated CCBA cross section of the 0_g^+ state, compared with experiment.

CCBA 0_g^+ cross section differs very little from that of DWBA. This means that the two-step and multistep processes are not important for the 0_g^+ cross section. The reason for this lies in the fact that the $L=2$ form factors that are responsible for the lowest multistep processes are rather small as compared with that of the direct, $L=0$ transition.

B. 2_1^+ cross section

In Fig. 5 we present various CCBA cross sections corresponding to various choices of form factors, together with that of DWBA as well as experiment. $\beta_2 = 0.13$ is used for the triton-channel deformation parameter. Some remarks may be given on the results obtained: (i) The DWBA cross section is smaller by about a factor 6 than the observed cross section. The fit of the shape of the calculated cross section to experiment is also not good, thus DWBA fails to explain the observed data; (ii) the CCBA cross sections that are obtained by including only one form factor of either the $0_g^+-0_g^+$ or the $2_1^+-2_1^+$ transition can account almost for the entire observed cross section, although the fit is not very good; (iii) the CCBA cross section which includes all of the form fac-

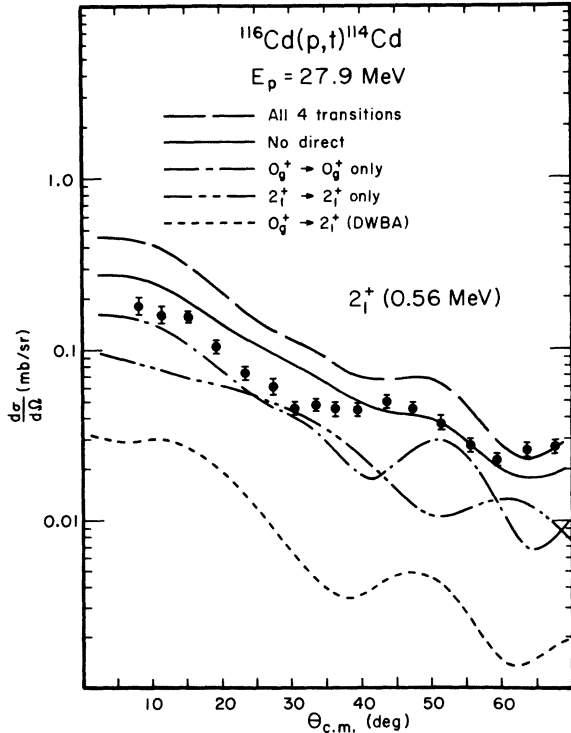


FIG. 5. Various calculated CCBA cross sections for the 2_1^+ state. $\beta_2 = 0.13$ is used for the triton optical-potential-deformation parameter. The calculated results are compared with experiment.

tors of set II, which ignores the direct transition form factor, reproduces very well the observed cross section. This implies that the 2_1^+ cross section can be explained only in terms of the multi-step processes; (iv) if we take into account the direct transition, i.e., if one uses the set I form factors, keeping the deformation parameter to be the same, the calculated CCBA cross section becomes slightly too large as compared with experiment.

This discrepancy, however, is remedied if use is made of $\beta_2 = 0.09$ (the set I) for the $0_g^+ - 2_1^+$ inelastic transition in the triton channel. To show this, we present in Fig. 6 the CCBA cross section obtained by using the form factor and the deformation parameter set I-I, together with that of II-II. We see that the calculated CCBA cross sections for both sets can reproduce almost equally the observed cross section.

As is clearly seen in the results of Fig. 5, the interference between the direct and indirect multi-step processes is constructive. A similar constructive interference was also observed in the 2_1^+ cross section of the $^{142}\text{Nd}(p, t)^{140}\text{Nd}$ reaction.¹⁸ On the other hand, we found a destructive interference in the case of $^{144}\text{Nd}(p, t)^{142}\text{Nd}$. These observations, together with the help of the RPA wave functions, enable us to understand the rather general behavior of the interference phenomena, which will be discussed in the next section.

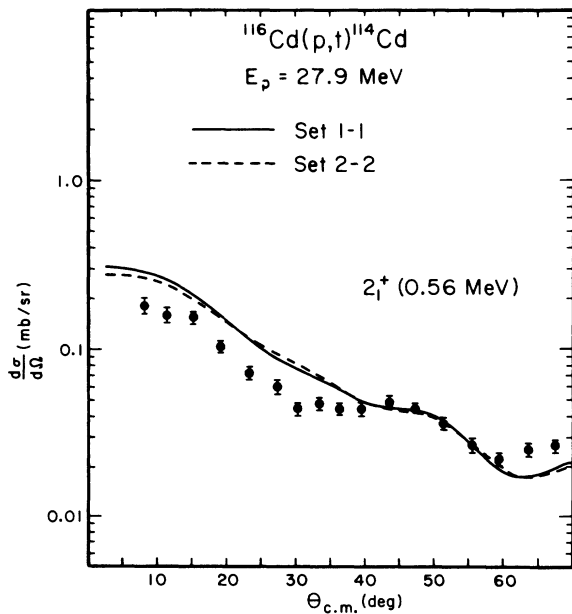


FIG. 6. Calculated CCBA cross sections of the 2_1^+ state for the form factor and the deformation parameter set I-I and II-II, compared with experiments.

C. 0_1^+ cross section

The CCBA calculations of the 0_1^+ were performed for both sets of the parameters I-I and II-II which reproduce the observed 2_1^+ cross section equally well. The results were presented in Fig. 7, together with the experimental data. The angular pattern of the observed cross section, which is quite different from that of 0_g^+ , is reproduced very well in the calculations of both sets of parameters. The fit is, however, slightly better for the set I-I. Also, it is remarkable that the observed magnitude of the cross section is explained very well by the calculations.

Since the above CCBA calculations include no direct (p, t) excitation, the calculated cross section comes entirely from the multistep processes. We want now to show that the major contribution to the cross section comes from the three-step and higher order multistep processes. To do this, we tried to calculate the cross section, neglecting all possible simple two-step processes, namely the $0_g^+ - 2_1^+$ form factor as well as direct $0_g^+ - 0_1^+$ inelastic excitations in both the incident and final nucleus channels. The results obtained in this way are shown in Fig. 8 and compared with the full CCBA cross sections obtained before. As is seen, the full CCBA cross section and the cross section

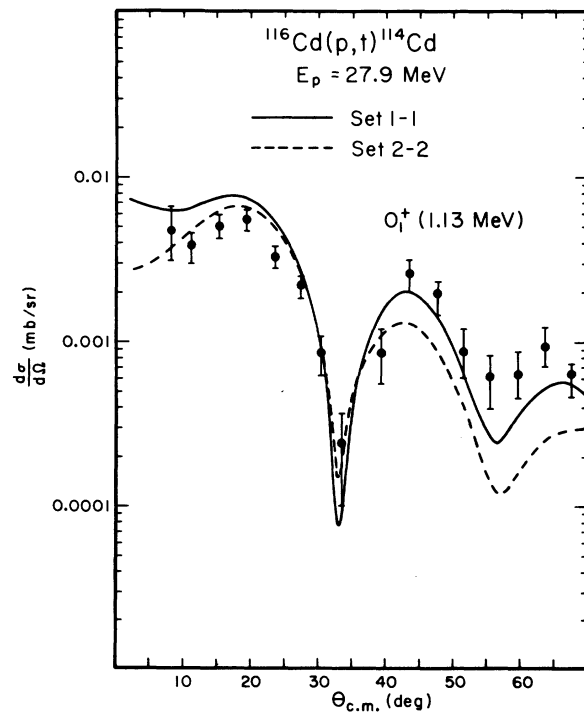


FIG. 7. Calculated CCBA cross sections of the 0_1^+ states for the two sets of form factors and deformation parameters. The results are compared with experiment.

in which the two-step processes are excluded differ very little from each other, indicating that the 0_1^+ cross section mainly comes from the three-step and higher multistep processes.

There are three important three-step processes, which come from the $0_g^+-0_g^+$, $2_1^+-2_1^+$, and $0_1^+-0_1^+$ (p, t) transitions. We studied contributions arising from each of the processes separately, finding that all these contributions are almost equally important: Thus, the neglect of any one of them destroys the fit that we obtained already, particularly the fit to the angular distributions.

As was already pointed out in Sec. II, the 3 0_1^+ cross sections involving 3 different target nuclei differ markedly from each other in both the shape and magnitude. This seems to suggest that the details of the 0_1^+ wave function change with the mass number. Phenomenologically this change in the wave function may be described by modifying some of the basic form factors and/or introducing some other form factors which are not in the basic set. Indeed, the observed change in the cross sections can rather easily be interpreted if we introduce the direct, $0_g^+-0_1^+$ (p, t) transition, which was neglected in the earlier calculations of the $^{116}\text{Cd}(p, t)^{114}\text{Cd}$ reaction. To demonstrate this, we did

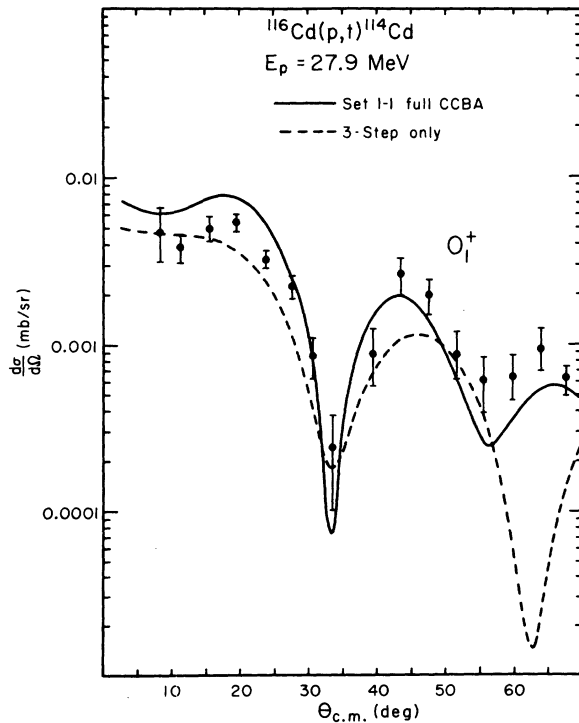


FIG. 8. Comparison of 2 CCBA cross sections for the 0_1^+ states; one is the full CCBA cross section while the other is the CCBA cross section obtained by including only the three-step processes; i.e., β' and β'' were set zero for both incident-proton and final-triton channels.

a CCBA calculation for the $^{114}\text{Cd}(p, t)^{112}\text{Cd}$ reaction including a direct transition, which is 10% of the $0_g^+-0_g^+$ (p, t) transition. The results obtained in this way are shown in Fig. 9, together with those for the $^{116}\text{Cd}(p, t)^{114}\text{Cd}$ reaction, as well as experiment. As is clearly seen in the figure, the inclusion of the direct transition mentioned above explains nicely the observed cross section for the $^{114}\text{Cd}(p, t)^{112}\text{Cd}$ reaction, and thus the observed change in the cross sections between the different targets.

It might be of value to note here that the above success is obtained since we assumed the same sign of the form factor as that of the $0_g^+-0_g^+$ transition. If the sign is reversed, the resultant CCBA cross section becomes very different from what we obtained before and thus the observed features can no longer be explained.

D. 2_2^+ cross section

We present in Fig. 10 the calculated CCBA cross sections obtained for the two sets of form factors and the deformation parameters used before. They are also compared with experiments. For the sake of reference, we plotted in this figure also the

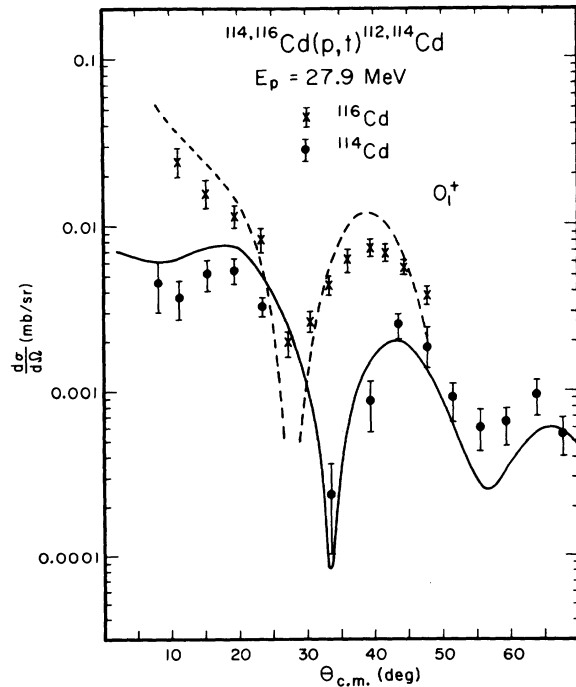


FIG. 9. Calculated CCBA cross sections of the 0_1^+ states. The full curve is that of Fig. 7, while the dotted curve is that obtained by including the form factor for the direct $0_1^+-0_1^+$ transition. The assumed form factor is 10% of the form factor of the $0_g^+-0_g^+$ transition. Relevant data are also shown.

cross sections for the 2_1^+ state, already given in Fig. 5. Both the shape and the magnitude of the observed cross section are seen to be reproduced very well in both types of calculations. It is particularly remarkable that the very marked difference between the shapes of the observed cross sections of the 2_1^+ and 2_2^+ are explained very well. Of course, the above difference between the two 2^+ cross sections cannot be explained by DWBA.

As was remarked in the last paragraph in Sec. II, the 2_2^+ state has a cross section which is much larger (by about a factor 5) than the cross sections of other two two-phonon states. We observe a similar situation in the inelastic scatterings, in which the observed 2_2^+ cross section is larger, say by about a factor 2, than those of other two two-phonon states.²²

This particular large cross section for the 2_2^+ state was explained in the inelastic scattering case as resulting from a rather strong direct $0_g^+-2_2^+$ inelastic excitation.²² Now, we want to show that this is also the case for the present (p, t) reaction; indeed, if we do the CCBA calculation without including the direct inelastic excitation mentioned above we can hardly explain the large cross section observed any more. To show this, we present in Fig. 11 the calculated CCBA cross section obtained by neglecting the above direct inelastic scattering processes, and also

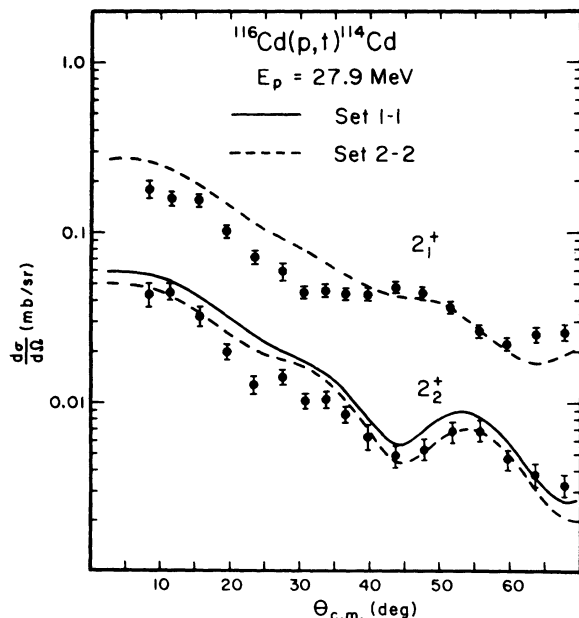


FIG. 10. Calculated CCBA cross sections of 2_2^+ states. The results are compared with experiment, as well as the calculated and observed 2_1^+ cross sections.

by including only the direct inelastic scattering process, together with the full CCBA cross section of Fig. 10. It is seen that the CCBA cross section, which neglects the direct inelastic scattering processes is smaller by about a factor 6 than that of full CCBA: This implies that the direct excitation effect is amplified in the (p, t) reaction case. This is due to a coherent effect of the direct excitations in both the incident-proton and exit-triton channels.

The CCBA calculation which includes only the direct inelastic excitation and neglects the $0_g^+-2_1^+$ and $2_1^+-2_2^+$ inelastic scattering processes explains almost the entire cross section observed. Thus, in contrast to the 0_1^+ state, the cross section of this 2_2^+ state comes mainly from the two-step processes.

E. 4_1^+ cross section

Three types of CCBA calculations were made for the 4_1^+ cross section, assuming the set I-I and II-II and also the set I-I plus a small form factor for the direct transition, $F_4(0_g^+-4_1^+)$, respectively. The form factor for the direct transition was obtained by using the G_N factor calculated for $^{142}\text{Nd}(p, t)^{140}\text{Nd}$ leading to the 1.8-MeV 4^+ state.²⁸

The cross sections thus obtained are plotted in Fig. 12, together with the experimental data. We plotted two experimental cross sections, one is

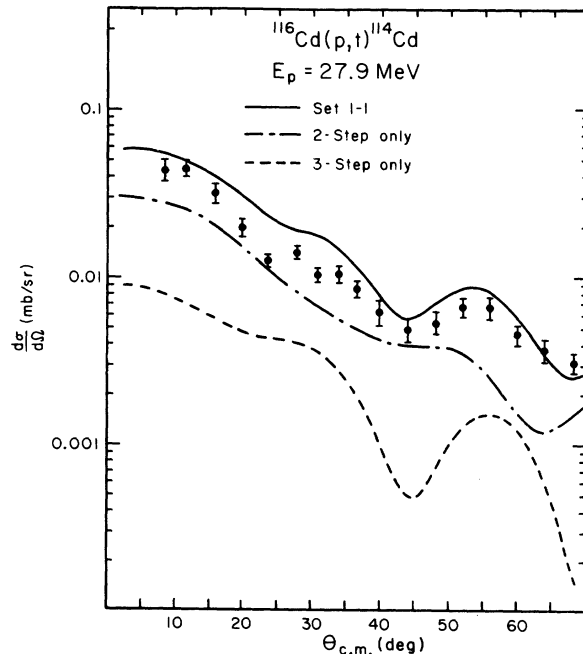


FIG. 11. Comparison of three CCBA cross sections of the 2_2^+ state; one is the full CCBA cross section, and the other two are those obtained by including only the three-step and the two-step processes, respectively.

that of $^{116}\text{Cd}(p, t)^{114}\text{Cd}$ and the other is an average of the cross sections taken for 3 different target nuclei, since the 4_1^+ state is actually a doublet and the observed cross section involves a contribution from the excitation of another doublet (0^+) state. The observed cross section, particularly the magnitude, is well reproduced in all of the calculations of Fig. 12.

However, the fit of the calculated angular distribution with experiment is not so good as compared with the fit we obtained for other two-phonon states. Note, however, that the fit is significantly improved if the direct process is included in the calculation. This might suggest that there is a possibility that the fit will be further improved by introducing other form factors and/or adjusting some of the parameters involved in the calculations.

We made a similar study of the effects of the two-step and three-step contributions as that made for the 0_1^+ and 2_2^+ states, finding that for this case the main contribution comes from three-step processes. The situation is the same as that of the 0_1^+ state. This is consistent with the fact that the observed magnitude of the cross sections are almost the same for both cases.

VI. FINAL REMARKS

A CCBA analysis is made of the $^{116}\text{Cd}(p, t)^{114}\text{Cd}$ reaction, leading to the ground, one-phonon, and two-phonon states of the final residual nucleus.

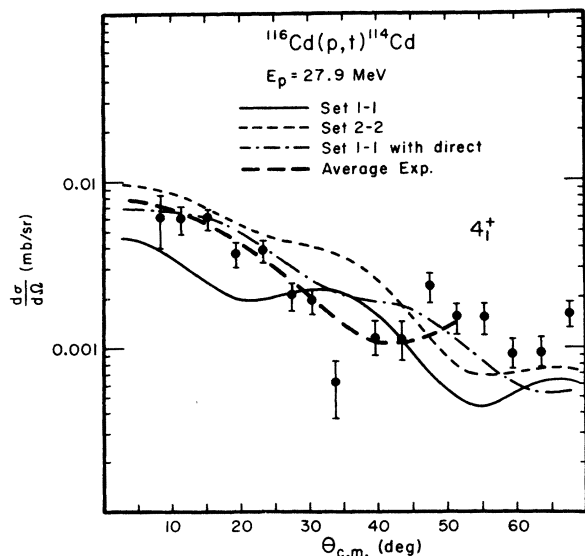


FIG. 12. Various calculated CCBA cross sections of the 4_1^+ state, compared with experiment. The average cross section is that obtained by taking the average of the 4_1^+ cross sections observed in 3 reactions.

Perhaps the most important conclusion obtained in this work is that CCBA does describe very well the (p, t) excitation of the two-phonon states. In fact we have seen that a number of the observed facts, which defy explanation by DWBA, can readily be explained by CCBA. It was also shown that the dominant contribution to the two-phonon cross sections comes from the three-step processes for the 0_1^+ and 4_1^+ states, but the two-step process is the most important for the 2_2^+ state.

In the present calculations, we neglected almost all the form factors associated with the two-phonon states, i.e., the form factors for the direct (p, t) excitations from the ground and the one-phonon states to the two-phonon states. We have found, however, that we can reproduce the observed data consistently this way. This may show that the form factors neglected in the present calculations are indeed quite small.

As was already remarked, this smallness of the form factors can be considered to result from two conditions: (i) The two-phonon state is essentially a four-quasiparticle state, so that the direct transition from the ground to the two-phonon state is forbidden^{8,12}; (ii) the (p, t) creation of a phonon is very unlikely for reactions such as those considered here. Under such circumstances it would be natural to expect that the (p, t) transition from one-phonon state is also weak.

It should be remarked, however, that the above two conditions may sometimes be violated. Indeed we needed, as was shown above, to introduce the direct $0_g^+ - 0_1^+$ (p, t) transition to explain the observed 0_1^+ cross section of the $^{114}\text{Cd}(p, t)^{112}\text{Cd}$ reaction, while such was not needed in order to explain a similar 0_1^+ cross section of $^{116}\text{Cd}(p, t)^{114}\text{Cd}$. The direct $0_g^+ - 0_1^+$ (p, t) transition may possibly arise if the BCS vacuum state or a two-quasiparticle state (such as a pairing-vibrational state) is mixed into the two-phonon state. This is certainly a violation of the condition (i), mentioned above.

The condition (ii) might be violated for target nuclei with neutron numbers which are somewhat different from what we considered in this work, so that the pairing and particle-hole correlations interfere more strongly. In such cases, the one-phonon to two-phonon (p, t) transitions may not be negligible anymore. It may thus be very interesting to perform a similar analysis for other cases of reactions involving different target nuclei.

Though the main objective of the present analysis was to test whether CCBA can successfully describe the (p, t) excitation of the two-phonon states of vibrational nuclei, we summarize in the rest of this section the results of the calcula-

tions on the ground and one-phonon states.

The ground-state cross section was very well reproduced by the DWBA as well as CCBA calculations. The zero-range constant D_0 needed to reproduce the observed cross section was found to be $D_0^2 = 4.8 \times 10^4 \text{ MeV}^2 \text{ fm}^3$, which is smaller than the value determined before.²⁹ This, however, seems to be reasonable since in the work of Ref. 29 the single-particle states in only one major shell were considered.

The one-phonon 2_1^+ cross section was also reproduced well by CCBA, but not by DWBA; the DWBA cross section was found to be too small to explain the observed cross section. This implies that the 2_1^+ cross section comes mainly from a multistep process, rather than the direct process; indeed it was shown that the 2_1^+ cross sections were explained without taking into account any direct contribution.

The interference between the direct and indirect multistep processes was found to be constructive in the present cases studied. A similar interference was also found in $^{142}\text{Nd}(p, t)^{140}\text{Nd}$ (see Ref. 18), while a destructive interference was found in $^{144}\text{Nd}(p, t)^{142}\text{Nd}$, as was already noted.⁴ Let us keep in mind these observations and also assume that the dependence of the interference on kinematic terms such as the incident energy, the reaction Q value, the target mass, and so on is rather weak, so that if the dynamical condition is the same, we obtain the same interference. Then, we can draw a rather general conclusion about the occupation-number dependence of the interference. Namely, the interference is destructive for (p, t) reactions from target nuclei in the beginning of the closed shell [$^{144}\text{Nd}(p, t)^{142}\text{Nd}$ is such a case], and by increasing the number of neutrons in the open shell, the interference becomes constructive

for some number of neutrons and then the constructive nature continues as the shell is closed.

The dynamical element that determines the constructive or destructive nature of the interference is the relative sign of the $L=0$, $0_2^+-0_1^+$ and $L=2$, $0_2^+-2_1^+$ form factors (in the asymptotic region) under a fixed-phase convention. The phase of the wave function is determined in such a way that we always have a positive (transition) deformation parameter and also a positive value of $L=0$ form factor in the asymptotic region. Then, utilizing the RPA wave function, it is easy to see that the sign changes at some neutron number in the middle of the closed shell region. This change of the sign results from a competition between two contributions coming from the forward and backward amplitudes in the RPA wave functions. At the beginning of the closed shell, the backward amplitude contribution exceeds that from the forward amplitude, while at the end of the closed shell the situation reverses. The backward amplitude describes the effect of the ground-state correlation, which contributes constructively to the $E2$ transitions, resulting in a strong enhancement. In the case of a (p, t) or a (t, p) reaction the effect is just opposite, contributing destructively to the main term.³⁰

The author should like to thank Professor J. R. Comfort and Professor W. J. Braithwaite for making their data available to him before publication and also for their kind interests in this work. This work was done in a close contact with Professor T. Tamura, to whom the author is grateful for his many stimulating discussions and suggestions. The author also wants to express his gratitude to Professor W. R. Coker for his careful reading of the manuscript and for many suggestions.

*Supported in part by U. S. Atomic Energy Commission.

¹R. A. Broglia, O. Hansen, and C. Riedel, *Advances in Nuclear Physics*, edited by M. Baranger and E. Vogt (Plenum, New York, 1973), Vol. 6.

²C. L. Lin and S. Yoshida, *Prog. Theor. Phys.* **32**, 885 (1964); N. K. Glendenning, *Phys. Rev.* **137**, B102 (1965).

³M. A. Othoudt and N. M. Hintz, to be published.

⁴K. Yagi, K. Sato, Y. Aoki, T. Udagawa, and T. Tamura, *Phys. Rev. Lett.* **29**, 1334 (1972).

⁵W. R. Falk, P. Kulisic, and A. McDonald, *Nucl. Phys.* **A167**, 157 (1971); J. R. Shepard, J. J. Kraushaar, and H. W. Baer, *Phys. Rev. C* **5**, 1288 (1972); R. S. Ohanian and G. T. Garvey, private communication.

⁶S. K. Penny and G. R. Satchler, *Nucl. Phys.* **53**, 145 (1964).

⁷R. J. Ascutto and N. R. Glendenning, *Phys. Rev.* **181**, 1396 (1969); and *Phys. Rev. C* **2**, 1260 (1970).

⁸N. K. Glendenning, in *Proceedings of the International Conference on Properties of Nuclear States, Montréal, Canada, 1969*, edited by M. Harvey *et al.* (Université de Montréal, Montréal, Canada, 1969), p. 245; R. J. Ascutto and N. K. Glendenning, *Phys. Rev. C* **2**, 415 (1970).

⁹R. J. Ascutto, N. R. Glendenning, and B. Sorensen, *Nucl. Phys.* **A183**, 60 (1972); and *Phys. Lett.* **34B**, 17 (1971).

¹⁰T. Tamura, D. R. Bes, R. A. Broglia, and S. Landowne, *Phys. Rev. Lett.* **25**, 1507 (1970); and **26**, 156(E) (1971).

¹¹D. K. Olsen, T. Udagawa, T. Tamura, and R. E. Brown, *Phys. Rev. Lett.* **29**, 1178 (1972); and *Phys. Rev. C* **8**, 609 (1973).

¹²J. R. Comfort, W. J. Braithwaite, J. R. Duray, and S. Yoshida, *Phys. Rev. Lett.* **29**, 442 (1972); and private communication.

- ¹³T. Tamura, *Rev. Mod. Phys.* **37**, 679 (1965); and *Ann. Rev. Nucl. Sci.* **19**, 99 (1969).
- ¹⁴See for instance W. T. Milner, F. K. McGowan, P. H. Stelson, R. L. Robinson, and R. O. Sayer, *Nucl. Phys.* **A129**, 689 (1969).
- ¹⁵Y. Kawase, K. Okano, S. Uehara, and T. Hayashi, *Nucl. Phys.* **A193**, 204 (1972).
- ¹⁶J. B. Ball, R. L. Auble, R. M. Driskol, and P. G. Roos, *Phys. Rev.* **177**, 1699 (1969); R. L. Auble and J. B. Ball, *Nucl. Phys.* **A179**, 353 (1972).
- ¹⁷S. Yoshida, *Nucl. Phys.* **33**, 685 (1962).
- ¹⁸T. Udagawa, T. Tamura, and T. Izumoto, *Phys. Lett.* **35B**, 129 (1971).
- ¹⁹We included in the actual calculations higher p-h phonon states, but these are neglected in Eq. (3), since they are not important for the purpose of the present form factor calculation. Note that due to this reason the sum of the squares of the amplitude is not 1.0.
- ²⁰D. G. Fleming, M. Blann, and H. W. Fulbright, *Nucl. Phys.* **A163**, 401 (1971).
- ²¹F. D. Becchetti, Jr. and G. W. Greenlees, *Phys. Rev.* **187**, 1190 (1969).
- ²²P. H. Stelson, J. L. C. Ford, Jr., R. L. Robinson, C. Y. Wong, and T. Tamura, *Nucl. Phys.* **A119**, 14 (1968).
- ²³J. A. Deye, R. L. Robinson, and J. L. C. Ford, Jr., *Nucl. Phys.* **A180**, 449 (1972).
- ²⁴D. Tweeton and C. Poppe, John H. Williams Laboratory of Nuclear Physics Annual Report, 1971 (unpublished), p. 133.
- ²⁵J. B. Ball, R. L. Auble, R. M. Drisko, and P. G. Roos, *Phys. Rev.* **177**, 1699 (1969).
- ²⁶N. Austern, *Direct Nuclear Reaction Theories* (Wiley, New York, 1969).
- ²⁷T. Tamura and T. Udagawa, University of Texas Center for Nuclear Studies Technical Report No. 3, 1972 (unpublished).
- ²⁸The state has a large cross section and thus can be considered as 4^+ type of the pairing-vibrational state. The G_γ factors were thus calculated by using the wave function obtained in RPA.
- ²⁹R. A. Broglia, C. Riedel, and T. Udagawa, *Nucl. Phys.* **A184**, 23 (1972).
- ³⁰R. A. Broglia, C. Riedel, and T. Udagawa, *Nucl. Phys.* **A167**, 401 (1971).